jove

Analyzing the Parkinson's Disease Mouse Model Induced by Adeno-associated Viral Vectors Encoding Human α-Synuclein

Daniela Elgueta[1], **Ornella Chovar**[1], **Valentina Ugalde**[1], **Vanesa Sánchez-Guajardo**[1], **Alejandra Catenaccio**[2], **Felipe Court**[2,3,4], **Rodrigo Pacheco**[1,5]

[1] Laboratorio de Neuroinmunología, Fundación Ciencia & Vida [2] Center for Integrative Biology, Universidad Mayor [3] FONDAP Geroscience Center for Brain Health and Metabolism [4] Buck Institute for Research on Ageing [5] Facultad de Medicina y Ciencia, Universidad San Sebastián

Corresponding Author

Rodrigo Pacheco
rpacheco@cienciavida.org

Citation

Elgueta, D., Chovar, O., Ugalde, V., Sánchez-Guajardo, V., Catenaccio, A., Court, F., Pacheco, R. Analyzing the Parkinson's Disease Mouse Model Induced by Adeno-associated Viral Vectors Encoding Human α-Synuclein. *J. Vis. Exp.* (185), e63313, doi:10.3791/63313 (2022).

Date Published

July 29, 2022

DOI

10.3791/63313

URL

jove.com/video/63313

Abstract

Parkinson's disease is a neurodegenerative disorder that involves the death of the dopaminergic neurons of the nigrostriatal pathway and, consequently, the progressive loss of control of voluntary movements. This neurodegenerative process is triggered by the deposition of protein aggregates in the brain, which are mainly constituted of α-synuclein. Several studies have indicated that neuroinflammation is required to develop the neurodegeneration associated with Parkinson's disease. Notably, the neuroinflammatory process involves microglial activation as well as the infiltration of peripheral T cells into the substantia nigra (SN). This work analyzes a mouse model of Parkinson's disease that recapitulates microglial activation, T-cell infiltration into the SN, the neurodegeneration of nigral dopaminergic neurons, and motor impairment. This mouse model of Parkinson's disease is induced by the stereotaxic delivery of adeno-associated viral vectors encoding the human wild-type α-synuclein (AAV-hαSyn) into the SN. The correct delivery of viral vectors into the SN was confirmed using control vectors encoding green fluorescent protein (GFP). Afterward, how the dose of AAV-hαSyn administered in the SN affected the extent of hαSyn expression, the loss of nigral dopaminergic neurons, and motor impairment were evaluated. Moreover, the dynamics of hαSyn expression, microglial activation, and T-cell infiltration were determined throughout the time course of disease development. Thus, this study provides critical time points that may be useful for targeting synuclein pathology and neuroinflammation in this preclinical model of Parkinson's disease.

Introduction

After Alzheimer's disease, Parkinson's disease is the second most prevalent neurodegenerative disease worldwide. The primary neurons affected in Parkinson's disease are those of the nigrostriatal pathway, which produce dopamine and control voluntary movement. As a consequence, the most characteristic symptom associated with this disorder is motor impairment. This pathology also involves the deposition of protein aggregates in the brain, which are composed mainly of α-synuclein (αSyn)[1], a cytosolic protein associated to presynaptic terminals. Evidence has shown that the generation of pathogenic inclusions of αSyn is triggered by misfolding or by some post-translational modifications of this protein[2].

Notably, a close relationship has been established between αSyn pathology and the loss of dopaminergic neurons of the nigrostriatal pathway in human Parkinson's disease and animal models[3,4]. Understanding how αSyn aggregates are generated and how they induce neuronal death represents a significant challenge in the field. A growing group of studies has shown that, by increasing oxidative stress, mitochondrial dysfunction is one of the leading causes for the generation of αSyn aggregates[2]. Indeed, several genes associated with Parkinson's disease risk encode proteins involved in mitochondrial function, morphology, and dynamics[5,6]. In addition, lysosomal dysfunction, which results in the accumulation of dysfunctional mitochondria and misfolded αSyn constitutes another major event promoting the generation of αSyn aggregates[7].

Emerging evidence has indicated that, once αSyn aggregates are deposited in the brain, these pathogenic proteins stimulate toll-like receptors (TLRs) on the microglia, thus triggering microglial activation and an initial inflammatory environment in the substantia nigra (SN)[8,9]. Furthermore, the evidence indicates that αSyn aggregates are captured and presented by antigen-presenting cells to T cells, inducing an adaptive immune response specific to αSyn[10,11]. These αSyn-specific T cells subsequently infiltrate the brain and are restimulated by activated microglia, thus promoting the secretion of neurotoxic factors that evoke neuronal death[9,10]. Interestingly, several lines of evidence have suggested that αSyn aggregates are generated first in the enteric nervous system and then transported through the vagus nerve to the brain stem[12].

Several animal models of Parkinson's disease have been used for many years, including those induced by the administration of neurotoxic substances (i.e., 6-hydroxydopamine, paraquat, rotenone, 1-methyl-4-phenyl-1,2,3,6-tetrahydropyridine) and those involving genetic conditions (i.e., mutant α-synuclein, mutant leucine-rich repeat kinase 2)[13]. Despite models involving neurotoxin-induced neurodegeneration replicating some aspects of Parkinson's disease, none of them recapitulate all the essential aspects of the disease or are not progressive[13]. On the other hand, although genetic mouse models involving the expression of mutant versions of leucine-rich repeat kinase 2, mutant versions of α-synuclein, or the overexpression of human wild-type α-synuclein result in motor impairment and, in some cases, also the development of synucleinopathy, they do not reproduce prominent neurodegeneration of the nigral dopaminergic neurons, which is an essential aspect of Parkinson's disease[13,14]. A third kind of animal model of neurodegeneration has managed to meet most of the essential aspects of Parkinson's disease, the stereotaxic

delivery of adeno-associated viral vectors (AAVs) encoding the human α-synuclein (AAV-hαSyn)[14,15]. Importantly, AAVs allow the transduction of neurons with high efficacy and in the long term in the adult brain of mammals. Furthermore, the stereotaxic delivery of AAV-hαSyn in the SN has been shown to reproduce many of the essential aspects of the disease, including αSyn pathology, microglial activation, neurodegeneration, and motor impairment[16,17,18,19,20]. This study presents an analysis of how the dose of viral vector and the time after viral vector delivery affects the extent of hαSyn expression, neurodegeneration, and neuroinflammation in the nigrostriatal pathway, as well as the degree of motor impairment in the mouse model of unilateral stereotaxic delivery of hαSyn in the SN.

Protocol

All studies were carried out under the 8th edition of the Guide for the Care and Use of Laboratory Animals. Experimental protocols were approved by the IACUC at the Fundación Ciencia & Vida (Science for Life Foundation), including those involving anesthesia, pain, distress, and euthanasia (Permit number P-035/2022).

1. The stereotaxic surgery

1. Preparation for the surgery (approximately 1 h)
    1. To maintain an aseptic environment, wear appropriate surgical clothes during the whole surgery, including shoe covers, a surgical mask, a sanitary barrier, gloves, and a surgical cap.
    2. Spray 70% ethanol on the mouse and all the surgical material to maintain an aseptic environment.
    3. To induce analgesia, inject the mouse with carprofen 5 mg/kg subcutaneously (s.c.) every 12 h[21] starting 1 h before the surgery and continuing until 3 days after the surgery.
    4. To anesthetize the mouse, place the animal in an induction chamber. Open the isoflurane flow at a rate of 0.5% and then slowly increase it up to 5% over approximately 5 min until the mouse has lost its righting reflex[22].
    5. Remove the animal from the induction chamber. Immediately transfer the animal to a non-rebreathing circuit with an appropriately sized nose cone. Maintain the mouse anesthesia with isoflurane 1% throughout the whole time of surgery.
    6. Confirm the mouse is entirely anesthetized by pinching its tail and paws. When the mouse does not react to pinching the tail and paws, it means the mouse is completely anesthetized.
    7. Shave the mouse's head using scissors. Clean the mouse's skin using a cotton swab with chlorhexidine 2% and remove all the hair.
    8. Fix the mouse's head in the stereotaxic frame.
    9. Place a corneal protectant in both mouse eyes using a cotton swab. To prevent stress induction in other rodents, avoid the presence of any other mouse in the surgery room[23].
2. The surgery (approximately 30 min)
    1. Clean the mouse's head with three rounds of 2% chlorhexidine followed by 70% ethanol. Expose the skull using surgical material and make a thin hole with a drill at the following coordinates: anteroposterior −2.8 mm, and mediolateral 1.4 mm with respect to the medial line.

2. Put the needle of a 10 µL syringe in the hole and move the needle inside the brain slowly until arriving at −7.2 mm dorsoventral with respect to the dura[24].
3. Leave the needle in the final position for 2 min to allow the tissue to settle a bit, and then inject 1 µL of AAV5-CBA-hαSyn (AAV-hαSyn), AAV5-CBA-eGFP (AAV-GFP), or vehicle (PBS at pH 7.4; sham surgery) into the right substantia nigra at a rate of 0.2 µL/30 s.
4. Leave the needle in the same position for 5 min after the delivery of viral vectors and then withdraw it slowly.

3. Post-surgery (approximately 5 min)
   1. Close the wound using a sterile silk-braided non-absorbable suture.
   2. Put the mouse in the home cage prewarmed by placing it over an electric heated mattress (25 °C).
      NOTE: The mouse must be maintained alone in the home cage until it is able to walk without difficulty and the wound has healed.

2. Determination of motor performance using the beam test

1. Training (approximately 15 min per mouse)
   1. Twelve weeks after the stereotaxic surgery, assess the motor performance using a simplified version of the beam test described before[25]. For this purpose, use a horizontal beam of 25 cm in length and 3 cm in width. The beam surface must be covered with a metallic grid with squares of 1 cm and elevated 1 cm above the beam.
   2. Take a video of the mouse traversing the grid-surface beam from one end to the opposite end of the beam, where the home cage is located. Train the mouse for 2 days before the determination of motor performance.
   3. On the first day, train the mouse to walk through the beam five times without the grid.
   4. On the second day, train the mouse to walk through the beam in the presence of the grid five times.
2. The test (approximately 5 min per mouse)
   1. On the third day, evaluate the motor performance. To do this, quantify the number of errors carried out by the left paws or by the right paws separately by watching the videos in slow-motion mode.
      NOTE: An error is defined as when a paw does not correctly step on the grid and, therefore, becomes visible on the side of the grid or between the grid and the beam surface.

3. Tissue processing

1. Transcardial perfusion (approximately 15 min per mouse)
   1. To anesthetize the mouse, inject a mixture of ketamine (80 mg/kg) and xylazine (10 mg/kg) intraperitoneally (i.p.) using a 1 mL syringe and 27 G needle[26].
   2. Once the mouse is completely anesthetized (confirmed as in step 1.1.6.), open the thorax with surgical material and expose the heart.
   3. Then, insert a 21 G needle (make the tip flat using a drill) into the heart's left ventricle.

4. By coupling the needle to a pipe, perfuse 50 mL of PBS (pH 7.4) at a rate of 9.5 mL/min using a peristaltic pump.

2. Fixing and cryoprotecting the brain (approximately 10 min per brain)
    1. Remove the brain using scissors and tweezers, and then fix it by immersion in 5 mL of 4% paraformaldehyde in PBS (pH 7.4) at 4 °C for 24 h.
    2. Afterward, put the fixed brain in 15 mL of 30% sucrose at 4 °C for 48 h.
    3. Then, put the brain in 4 mL of cryoprotection solution (20% glycerine and 2% DMSO in PBS) and save the brain at −80 °C or use it immediately in the next step.
3. Obtaining brain slices (approximately 20 min per brain).
    NOTE: Ensure that the brain is placed in a cryostat in a proper position to make coronal cuts.
    1. To obtain SN slices, cut the brain into 40 µm thick sections starting at −2.92 mm and finishing at −3.64 mm[24].
    2. Harvest each slice in a well (containing 1 mL of cryoprotection solution) of a 24-well plate following an anteroposterior order as described before[25,27,28].
    3. To perform immunohistochemical (section 4.) and immunofluorescence analyses (section 5.) in the SN, choose six coronal SN sections taken at uniform intervals (120 µm) that cover the entire rostrocaudal extent of the nucleus (720 µm in total), as described before[25,27,28].
    4. To obtain striatal slices, cut the brain into 40 µm thick sections starting at +1.34 mm and finishing at −0.26 mm[24].
    5. Harvest each slice in a 2 mL cryotube (containing 1 mL of cryoprotection solution) following an anteroposterior order.
    6. To perform immunohistochemical (section 4.) and immunofluorescence analyses (section 5.) in the striatum, choose five coronal striatal sections taken at uniform intervals (320 µm) that cover the entire rostrocaudal extent of the nucleus (1600 µm in total).

4. Immunohistochemical analysis to quantify dopaminergic neurons and microgliosis (approximately 2 days)

1. For immunohistochemical analysis of striatal or nigral slices, place the set of five (striatum) or six (SN) slices from the same brain in one well of a 24-well plate.
2. Wash the sections 3x with 1 mL of PBS and then incubate with 0.5 mL of 0.03% H_2O_2 in methanol at room temperature and with agitation for 30 min to inactivate endogenous peroxidase activity.
3. Wash the sections 3x with 1 mL of PBS and incubate with 0.5 mL of blocking solution (4% goat serum, 0.05% Triton X-100, and 4% BSA in PBS) at room temperature and with agitation for 40 min.
4. Afterward, incubate with 0.5 mL of blocking solution containing the primary antibody (rabbit anti-tyrosine hydroxylase [TH] pAb diluted 1:1000 [see **Table 1**]; or rabbit anti-Iba1 antibody diluted 1:1000) at room temperature and with agitation overnight.
5. Wash the sections 3x with 1 mL of PBS and incubate with 0.5 mL of blocking solution containing biotinylated goat

anti-rabbit pAb (1:500, see **Table 1**) at room temperature and with agitation for 2 h.

6. Then, wash the sections 3x with 1 mL of PBS and incubate with 0.5 mL of peroxidase-conjugated avidin (1:5000, see **Table 1**) in blocking solution at room temperature and with agitation for 90 min.

7. Wash the sections 3x with 1 mL of PBS and incubate with 0.5 mL of substrate solution (0.05% diaminobenzidine in 0.03% H_2O_2/Trizma-HCl buffer at pH 7.6). Wear gloves and a lab coat for this step, as diaminobenzidine is a potential carcinogen.

8. When the specific staining is evident (typically 30 sec for TH and 5 min for Iba1), take out the substrate solution and wash the sections 3x with 1 mL of PBS at room temperature and with agitation. Always carry out the immunostaining of slices of all the brains included in the same experiment simultaneously.

   NOTE: The specific staining of TH is evident when TH immunostaining appears in the area of the SN, which displays a characteristic shape in the brain. The specific mark of Iba1 is determined when Iba1 immunostaining appears on control brain slices with typical microglial shapes, which are confirmed upon microscope observation. In this way, the exact time of substrate exposition for IHC analysis is determined for every single experiment.

9. Mount the brain sections on glass slides using a solution of 0.2% gelatin in 0.05 M Tris (pH 7.6). Place each set of five (striatum) or six (SN) slices obtained from the same brain in rostrocaudal order on the same glass slide.

10. Quantify the number of TH^+ neurons in the SN.

    1. To quantify TH^+ neurons in the SN, acquire photos of the six slices at 20x magnification using a bright-field microscope, as described before[25,27,28]. Use the following adjust of color: color temperature 3200 K, cyan-red 40%, magenta-green 39%, yellow-blue 54%, gamma 0.5, contrast 37, brightness 13, saturation 5.

    2. Using the Image J software, select the perimeter of the SN pars compacta in the hemisphere analyzed. Avoid the selection of TH^+ neurons from the ventral tegmental area (VTA).

    3. Afterward, ask the software to calculate the area selected (typically 0.04-0.07 mm^2/hemisphere, depending on the rostrocaudal position). Then, using the multipoint tool, tag every single TH^+ neuron with a dot.

    4. Using the point tool, ask the software to count the total number of dots. With the number of total dots (TH^+ neurons) and the area of the SNpc, calculate the density of TH^+ neurons/mm^2.

    5. Repeat the same calculation in both hemispheres on the six SN slices and then calculate the mean of TH^+ neurons/mm^2 on the ipsilateral and the contralateral sides.

11. Quantify the number of activated microglia in the striatum

    1. To quantify activated microglia in the striatum, acquire two photos in each hemisphere for all five striatal slices at 20x magnification using a bright-field microscope and the same settings indicated in step 4.10.1. Using the Image J software, in every single photo (displaying an area of 660 µm x 877 µm), tag with a dot every single cell expressing high Iba1 intensity and ameboid shape using the multipoint

tool. Using the point tool, ask the software to count the total number of dots.

2. With the number of total dots and the area of the photo, calculate the density of activated microglia (Iba1^{high} cells/mm^2) as performed before[29].

Target antigen	Coupled to	Clonality	Host specie	Specie reactivity*	Dilution**
Tyrosine Hydroxylase	N/A	Polyclonal	Rabbit	Mouse, Rat, Human	1/200 - 1/1000
Iba1	N/A	Monoclonal	Rabbit	Mouse, Rat, Human	1/1000
alpha-Synuclein	N/A	Monoclonal	Rabbit	Human	1/150
CD4	N/A	Monoclonal	Rat	Mouse	1/250
IgG (H+L)	Biotinilated	Polyclonal	Goat	Rabbit	1/500
IgG (H+L)	AlexaFluor 546	Polyclonal	Goat	Rabbit	1/500
IgG (H+L)	AlexaFluor 647	Polyclonal	Goat	Rabbit	1/500
IgG (H+L)	AlexaFluor 546	Polyclonal	Goat	Rat	1/500

Table 1: Antibody dilutions. N/A, not applicable. *, It is only specified if there are reactivities with mouse, rat, and human, irrespective of the reactivity with other species. **, A single dilution or a dilution range is specified.

5. Immunofluorescence analysis to evaluate T cell infiltration in the nigrostriatal pathway (approximately 2 days)

1. For immunofluorescence analysis of hαSyn or TH/GFP on striatal or nigral slices, put together the set of five (striatum) or six (SN) slices from the same brain in one well of a 24-well plate.
    1. Wash the sections 3x with 1 mL of PBS and then incubate with 0.5 mL of blocking solution (0.3% Triton X-100, 0.05% tween20, and 5% BSA in PBS) at room temperature and with agitation for 40 min.
    2. Afterward, incubate with 0.5 mL of blocking solution containing the primary antibody (rabbit anti-TH pAb diluted 1:500; or rabbit anti-hαSyn antibody diluted 1:150, see **Table 1**) at room temperature and with agitation overnight.
    2. Wash the sections 3x with 1 mL of PBS and incubate with 0.5 mL of blocking solution containing AlexaFluor546-coupled anti-rabbit secondary antibody (1:500, see **Table 1**) and 4′,6-diamidino-2-phenylindole (DAPI; 1:1000) at room temperature and with agitation for 2 h. Then, wash the sections 3x with 1 mL of PBS.
    3. Mount the brain sections on glass slides as described above (step 4.9.). Images were acquired with an inverted fluorescence microscope coupled to a power supply unit.
    4. For immunofluorescence analysis of TH/CD4/GFP(Foxp3) on nigral slices, place the set of six (SN) slices from the same brain in one well of a 24-well plate. Wash the sections 3x with 1 mL of PBS and then incubate with 0.5 mL of blocking solution (0.5% Triton X-100, 0.5% fish skin gelatin in PBS) at room temperature and with agitation for 2 h.

5. Incubate with 0.5 mL of blocking solution containing the primary antibodies rabbit anti-TH pAb (1:200, see **Table 1**) and rat anti-CD4 (1:250) at 4 °C and with agitation overnight.
6. Wash the sections 3x with 1 mL of PBS and incubate with 0.5 mL of blocking solution containing anti-rabbit coupled to AlexaFluor 647 (1:500, see **Table 1**) and anti-rat coupled to AlexaFluor 546 (1:500) at room temperature and with agitation for 2 h. Then, wash the sections 3x with 1 mL of PBS.
7. Put each set of six (SN) slices obtained from the same brain in rostrocaudal order on the same glass slide and mount them using Fluoromount G. Acquire images using a Leica DMi8 microscope. Use the confocal microscope settings indicated in **Table 2** to acquire images from immunofluorescence analysis.

Chanel Name	Cube	Emission Wavelenght	Lookup Table name	Exposure time	Gain	Resolution XY	Resolution Z
Channel 1	Y5	700nm	Grey	1,011.727 ms	high well capacity	2.237 um	24.444 um
Channel 2	GFP	525nm	Green	326.851 ms	high well capacity	2.237 um	24.444 um
Channel 3	TXR	630nm	Red	406.344 ms	high well capacity	2.237 um	24.444 um
Channel 4	Dapi	460nm	Blue	91.501 ms	high well capacity	2.237 um	24.444 um

Table 2: Confocal microscope settings used for the acquisition of images from immunofluorescence analysis.

6. Statistical analysis

1. To compare data obtained from the ipsilateral and the contralateral sides, use a paired two-tailed Student's t-test.
2. To compare data obtained from mice receiving AAV-hαSyn and from mice receiving AAV-GFP or sham surgery, use an unpaired two-tailed Student's t-test. Consider significant differences when P values < 0.05.

Representative Results

Validating the correct delivery of AAV vectors in the dopaminergic neurons of the nigrostriatal pathway

To study the processes of neuroinflammation, neurodegeneration, and motor impairment promoted by synuclein pathology, a mouse model of Parkinson's disease induced by the unilateral stereotaxic delivery of AAV encoding hαSyn in the SN[16,17,30,31] was used (see the experimental design in **Supplementary Figure 1**). To validate the correct delivery of AAV vectors in the dopaminergic neurons of the nigrostriatal pathway, AAV encoding GFP (AAV-GFP) was

injected in the SN, and 12 weeks later, GFP fluorescence and tyrosine hydroxylase (TH) immunoreactivity were analyzed in the SN and striatum by immunofluorescence. The GFP-associated fluorescence was observed exclusively on the ipsilateral side, and there was significant colocalization with TH immunoreactivity in both the SN and striatum, indicating the correct delivery of AAV vectors in the dopaminergic neurons of the nigrostriatal pathway (**Figure 1**).

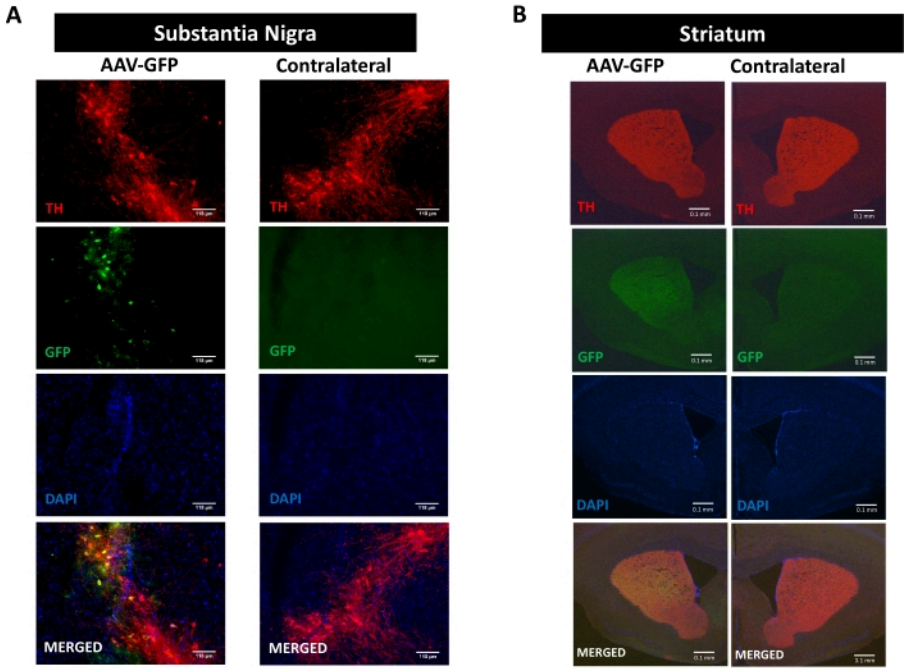

Figure 1: Analysis of the delivery of AAV-GFP in the nigrostriatal pathway. Mice received AAV-GFP (1 x 10^{10} vg/mouse) and 12 weeks later were sacrificed, and TH was immunostained in (**A**) the SN (scale bars are 118 µm) and (**B**) the striatum (scale bars are 100 µm). TH- and GFP-associated fluorescence were analyzed by epifluorescence microscopy. Nuclei were stained with DAPI. Representative images of merged or single staining of TH (red), GFP (green), and DAPI (blue) are shown. Please click here to view a larger version of this figure.

Setting up the dose of viral vector administered to induce neurodegeneration and motor impairment in the mouse model of Parkinson's disease induced by AAV-hαSyn

To test the dose of AAV-hαSyn required to induce a significant overexpression of hαSyn that promotes neurodegeneration of the nigral dopaminergic neurons, different doses (1 x 10^8 viral genomes [vg]/mouse, 1 x 10^9 vg/mouse, or 1 x 10^{10} vg/mouse) of AAV-hαSyn were injected, and 12 weeks later, hαSyn immunoreactivity and the extent of TH immunoreactivity were evaluated in the nigrostriatal pathway. Although hαSyn immunoreactivity was evident with all doses tested in the SN (**Figure 2**), only mice receiving 1 x 10^{10} vg/mouse presented evident hαSyn immunoreactivity in the striatum (**Figure 3**). Moreover, mice receiving 1 x 10^{10} vg/mouse of AAV-hαSyn displayed a significant loss of dopaminergic neurons in the SN (**Figure 4A**,**B**). Although

mice receiving 1 x 10^{10} vg/mouse of AAV-GFP displayed a low degree (~20%) of neuronal loss (**Figure 4A,B**), mice receiving the same dose of AAV-hαSyn presented a significantly higher degree of neurodegeneration of nigral dopaminergic neurons (**Figure 4C**). Accordingly, further experiments were performed using 1 x 10^{10} vg/mouse of AAV-hαSyn. In addition, the extent of motor impairment was determined in mice receiving different doses of AAV-hαSyn by using the beam test (**Figure 5A**), as described before[25]. A significant reduction in motor performance was detected exclusively with 1 x 10^{10} vg/mouse of AAV-hαSyn in the beam test both when comparing the number of errors made by the right and the left pads (**Figure 5B**) and when comparing the total number of errors of mice receiving AAV-hαSyn compared with mice receiving the control vector AAV-GFP (**Figure 5C**). Accordingly, further experiments were performed using 1 x 10^{10} vg/mouse of AAV-hαSyn.

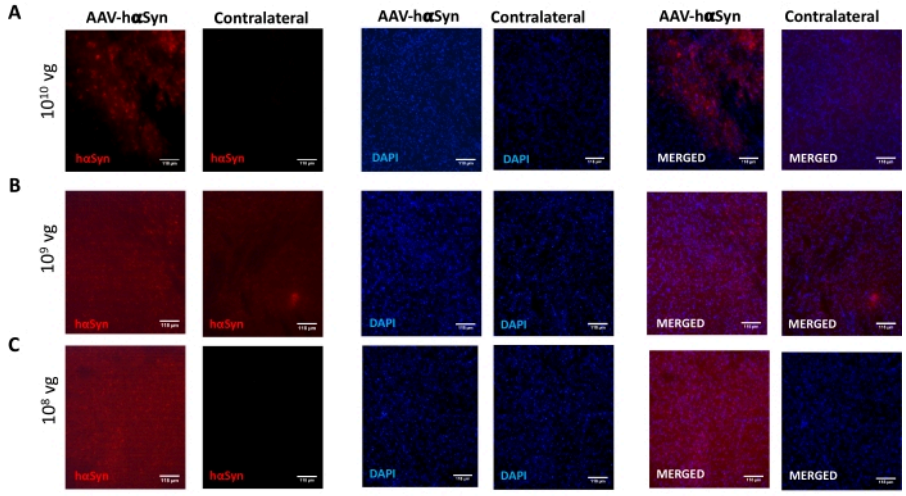

Figure 2: Analysis of human α-synuclein expression in the SN of mice treated with different doses of AAV-hαSyn. Mice received AAV-hαSyn at (**A**) 1 x 10^{10} vg/mouse, (**B**) 1 x 10^{9} vg/mouse, or (**C**) 1 x 10^{8} vg/mouse and 12 weeks later were sacrificed, and the hαSyn expression was analyzed by immunofluorescence in the SN using epifluorescence microscopy. Nuclei were stained with DAPI. Representative images of merged or single staining of hαSyn (red) or DAPI (blue) are shown. Scale bars are 118 µm. Please click here to view a larger version of this figure.

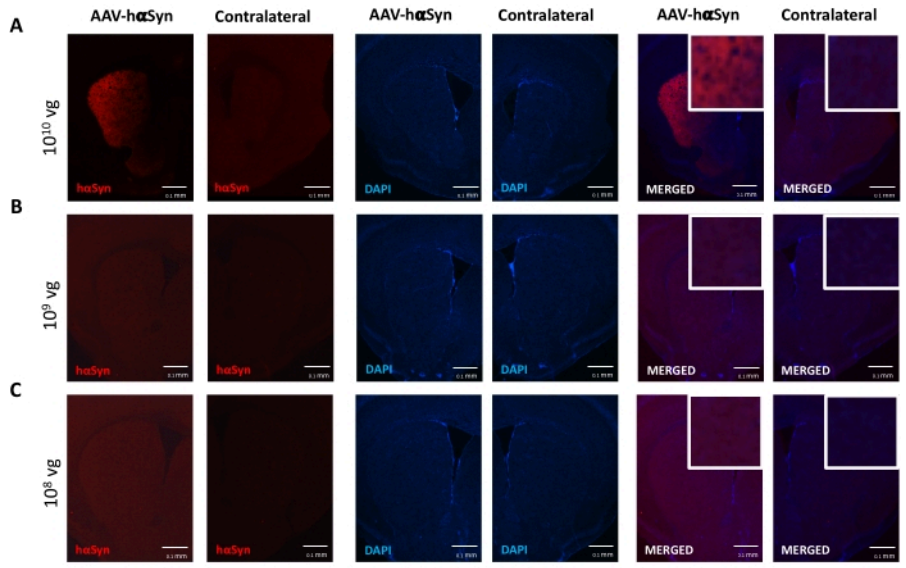

Figure 3: Analysis of human α-synuclein expression in the striatum of mice treated with different doses of AAV-hαSyn. Mice received AAV-hαSyn at (**A**) 1 x 10^{10} vg/mouse, (**B**) 1 x 10^{9} vg/mouse, or (**C**) 1 x 10^{8} vg/mouse) and 12 weeks later were sacrificed, and the hαSyn expression was analyzed by immunofluorescence in the striatum using epifluorescence microscopy. Nuclei were stained with DAPI. Representative images of merged or single staining of hαSyn (red) or DAPI (blue) are shown. Scale bars are 100 µm. The insert on the upper-right corner of the merged images shows an area of interest in higher magnification. Please click here to view a larger version of this figure.

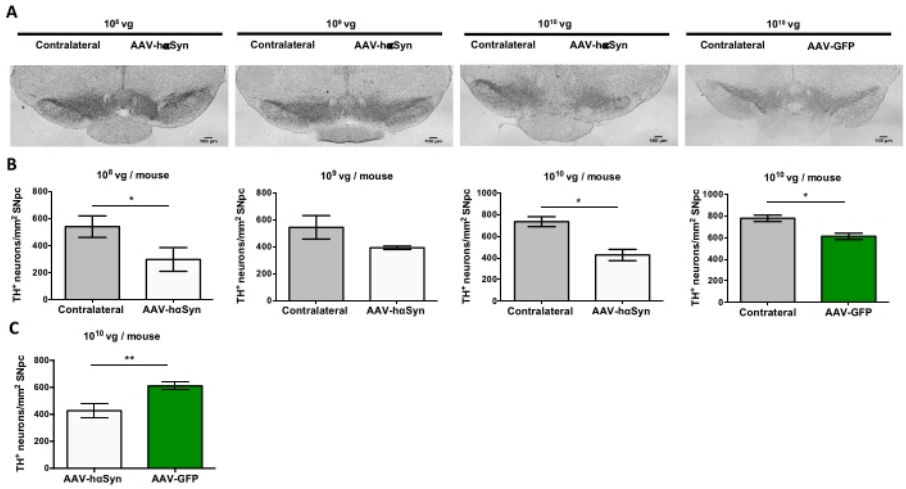

Figure 4: Loss of dopaminergic neurons of the SN in mice treated with different doses of AAV-hαSyn or control vector. Mice received AAV-hαSyn (1 x 10^{10} vg/mouse, 1 x 10^{9} vg/mouse, or 1 x 10^{8} vg/mouse) or AAV-GFP (1 x 10^{10} vg/mouse) and 12 weeks later were sacrificed, and TH was analyzed in the SNpc by immunohistochemistry. (**A**) Representative images. Scale bars, 100 µm. (**B,C**) The density of neurons was quantified as the number of TH+ neurons/mm^2. Data represent mean ± SEM. n = 3–8 mice per group. (**B**) A comparison of ipsilateral with contralateral sides was performed using the two-tailed paired Student's t-test. (**C**) A comparison of ipsilateral sides from mice receiving 1 x 10^{10} vg/mouse of AAV-hαSyn or AAV-GFP was carried out. (**B,C**) Whereas white bars indicate the quantification of TH+ neurons on the ipsilateral side of mice receiving AAV-hαSyn, green bars indicate the quantification of TH+ neurons on the ipsilateral side of mice receiving AAV-GFP. Grey bars indicate the quantification of TH+ neurons on the contralateral side of the corresponding group. Comparisons were performed by a two-tailed unpaired Student's t-test. *p < 0.05; **p < 0.01. Please click here to view a larger version of this figure.

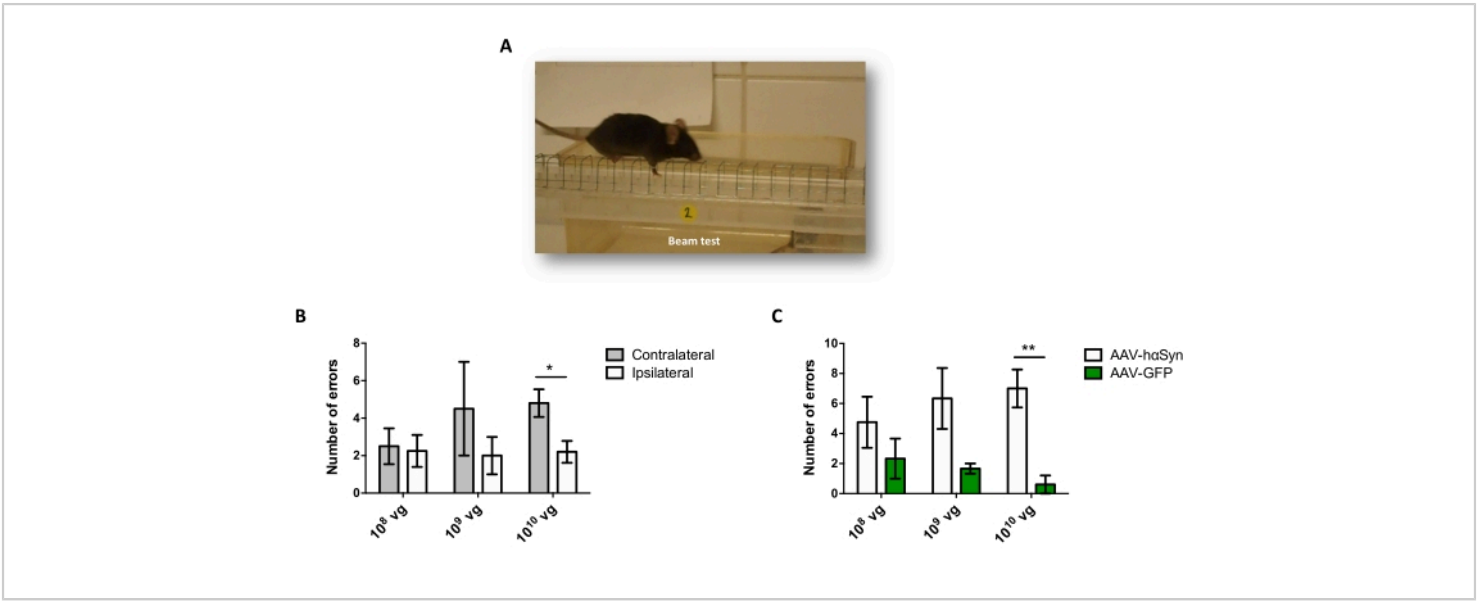

Figure 5: Analysis of the motor performance in mice treated with different doses of AAV-hαSyn. Mice received different doses (1 x 10^{10} vg/mouse, 1 x 10^9 vg/mouse, or 1 x 10^8 vg/mouse) of AAV-hαSyn or AAV-GFP, and 12 weeks later, the motor performance was evaluated by the beam test. (**A**) Image of a mouse walking on the beam. (**B**) The number of errors carried out by left limbs (contralateral) versus right limbs (ipsilateral) was quantified in the groups of mice receiving AAV-hαSyn. (**C**) The total number of errors was compared between different experimental groups receiving the same dose of AAV-hαSyn or AAV-GFP. Data represent mean ± SEM. n = 3–5 mice per group. Comparisons were performed by (**B**) a paired two-tailed Student's t-test or by (**C**) an unpaired two-tailed Student's t-test. *p < 0.05; **p < 0.01. Please click here to view a larger version of this figure.

Setting up the kinetics of the Parkinson's disease model induced by AAV-αSyn

After determining the proper AAV-hαSyn dose used to induce a significant level of neurodegeneration and motor impairment, experiments to define the onset of hαSyn overexpression were conducted. For this purpose, mice were treated with 1 x 10^{10} vg/mouse of AAV-hαSyn or sham surgery. The extent of hαSyn expression was analyzed in the SN once per week during weeks 2-5 after the stereotaxic surgery (see the experimental design in **Supplementary Figure 2**). The results show that, despite hαSyn expression being detected at low levels as early as 2 weeks after the surgery, hαSyn clusters appeared at week 5 after the stereotaxic surgery (**Figure 6**).

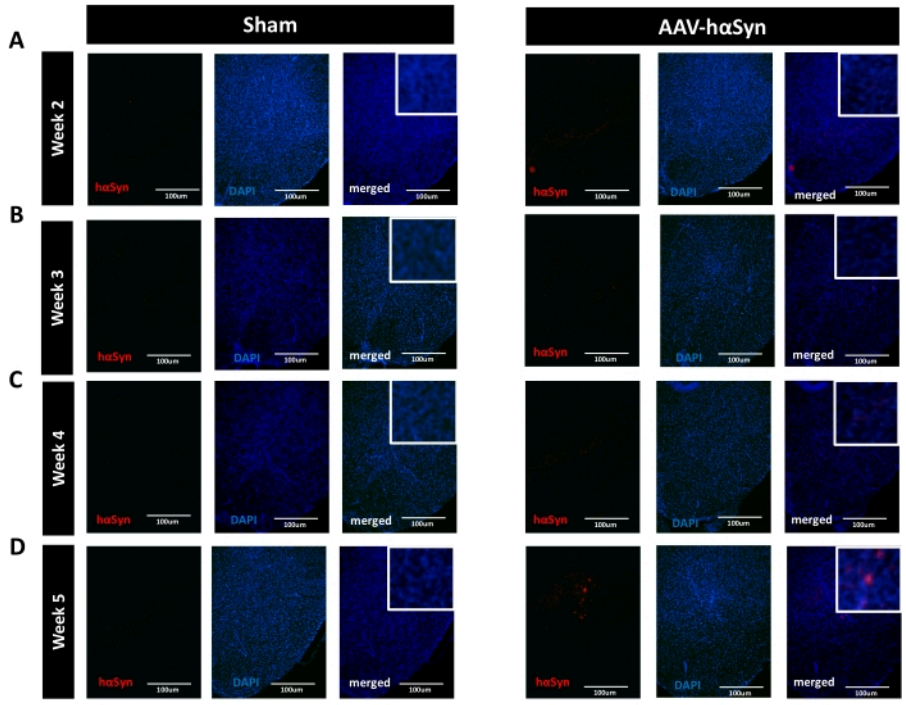

Figure 6: Analysis of the time course of human α-synuclein expression in the SN of mice treated with AAV-hαSyn. Mice received AAV-hαSyn (1 x 10^{10} vg/mouse) or just the sham stereotaxic surgery, and the expression of hαSyn in the SN was analyzed (**A**) 2 weeks, (**B**) 3 weeks, (**C**) 4 weeks, or (**D**) 5 weeks later by immunofluorescence using epifluorescence microscopy. Nuclei were stained with DAPI. Representative images of merged or single staining of hαSyn (red) or DAPI (blue) are shown. Scale bars, 100 µm. The insert on the upper-right corner of the merged images shows an area of interest in higher magnification. Please click here to view a larger version of this figure.

Afterward, experiments were conducted to determine the suitable time points to analyze neuroinflammation and T-cell infiltration in the central nervous system (CNS) after the stereotaxic delivery of AAV-hαSyn. To determine the peak of microglial activation after the treatment of mice with AAV-hαSyn, the extent of cells expressing high levels of Iba1 in the striatum was evaluated once per week during weeks 2-15 after the stereotaxic surgery. The results show a significant increase in microglial activation of the ipsilateral side compared with the contralateral side of mice 15 weeks after the AAV-hαSyn treatment (**Figure 7**). The number of Treg ($CD4^+$ $Foxp3^+$) cells infiltrated into the SNpc was also evaluated at different time points after the stereotaxic delivery of AAV-hαSyn by immunofluorescence followed confocal microscopy observation. The results show that the peak of Treg infiltration into the SNpc was at 11 weeks after surgery, whereas the extent of Treg infiltrating this area of the brain was lower at week 8 or week 13 after surgery (**Figure 8**). No $CD4^+$ T cells were detected infiltrating the striatum (data not shown). Altogether, these results indicate that, using 1 x 10^{10} vg/mouse of AAV-hαSyn, the most suitable time point to analyze neuroinflammation is week 15 after the

stereotaxic surgery, while a proper time point to analyze T-cell infiltration into the CNS seems to be week 11 after AAV-hαSyn treatment.

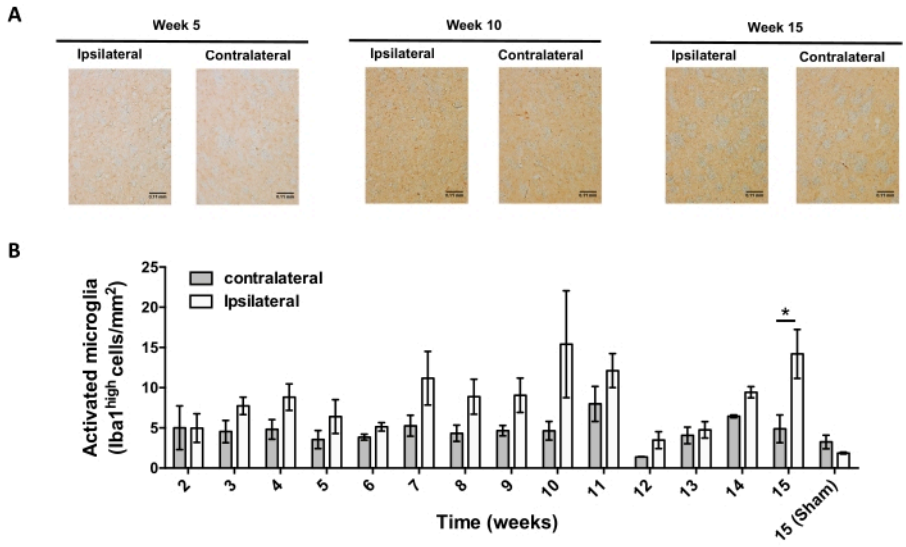

Figure 7: Analysis of the time course of microglial activation in mice inoculated with AAV-hαSyn. Mice received AAV-hαSyn (1 x 10^{10} vg/mouse), and microglial activation was evaluated by immunohistochemical analysis of Iba1 in the striatum at different time points after the surgery. (**A**) Representative overview images of immunohistochemical analysis of Iba1 from mice sacrificed 5 weeks, 10 weeks, or 15 weeks after inoculation with AAV-hαSyn are shown. Scale bars, 110 µm. (**B**) The density of activated microglia was quantified as the number of cells expressing high levels of Iba1 and ameboid shape per area. Data represent mean ± SEM. n = 3 mice per group. A two-tailed paired Student's t-test was used to determine statistical differences between ipsilateral and contralateral Iba1 in each group. *p < 0.05. Please click here to view a larger version of this figure.

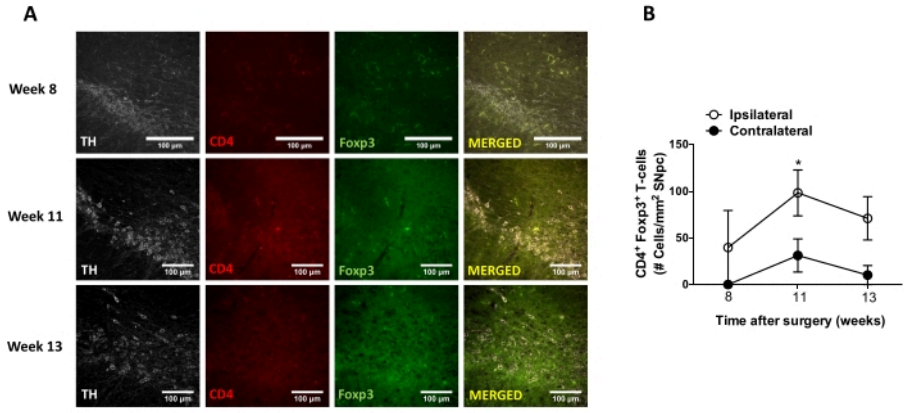

Figure 8: Analysis of the time course of CD4+ T-cell infiltration into the SN of mice inoculated with AAV-hαSyn. Foxp3^{gfp} reporter mice received AAV-hαSyn (1 x 10^{10} vg/mouse). The presence of CD4^{+} T-cells expressing Foxp3 and the presence of TH^{+} neurons were analyzed at different time points (week 8, week 11, and week 13 after the surgery) in the SN by immunofluorescence. (**A**) Representative images for single immunostaining or the merge are shown. Scale bars, 100 µm. (**B**) The number of CD4^{+} Foxp3^{+} T cells per area in the SN was quantified. Data represent mean ± SEM from 3 mice per group. *p<0.05, ipsilateral versus contralateral CD4^{+} Foxp3^{+} T cells by two-tailed Student's t-test. Please click here to view a larger version of this figure.

Supplementary Figure 1: Experimental design for evaluating the effect of different doses of AAV vectors on synuclein pathology, neurodegeneration, and motor impairment. Wild-type male C57BL/6 mice were anesthetized and received stereotaxic inoculation of different doses (1 x 10^{10} vg/mouse, 1 x 10^{9} vg/mouse, or 1 x 10^{8} vg/mouse) of AAV encoding human α-synuclein (AAV-hαSyn) or eGFP (AAV-GFP) under the control of the CBA promoter into the right substantia nigra (SN). After 12 weeks, the expression of GFP and hαSyn in the SN and striatum (Str) were evaluated by immunofluorescence (IF), tyrosine hydroxylase positive (TH+) cells were quantified by immunohistochemistry (IHC) in the SN, and motor performance was evaluated by the beam test. The number of mice in each experimental group is indicated in parenthesis. * indicates groups where one mouse died before the analyses. Each analysis indicates in parenthesis the number of the figure from the body of the paper where the corresponding results are shown. Please click here to download this File.

Supplementary Figure 2: Experimental design for determining the kinetics of T-cell infiltration, neuroinflammation, and hαSyn expression. Foxp3^{gfp} reporter mice were anesthetized and received stereotaxic inoculation of AAV (1 x 10^{10} vg/mouse) encoding human α-synuclein (AAV-hαSyn) under the control of the CBA promoter into the right substantia nigra (SN) or sham surgery (PBS). Mice were sacrificed at different time points, and the expression of hαSyn in the SN and striatum was evaluated by immunofluorescence (IF), GFP (Foxp3), CD4, and tyrosine hydroxylase positive (TH^{+}) cells were quantified

by IF in the SN, and Iba1 expression was analyzed by immunohistochemistry (IHC) in the striatum (Str). The number of mice in each experimental group is indicated. The range of time points included in each analysis is indicated. Each analysis indicates in parenthesis the number of the figure from the body of the paper where the corresponding results are shown. Please click here to download this File.

Discussion

The mouse model of neurodegeneration analyzed here might help study many critical aspects involved in the pathophysiology of Parkinson's disease, including the mechanisms involved in αSyn pathology and microglial activation, the involvement of the peripheral immune system in the regulation of neuroinflammation, and the mechanisms of neurodegeneration. Among the mechanisms involved in αSyn pathology are those subcellular mechanisms associated with mitochondrial, lysosomal, or proteasomal dysfunction in the presence of an excessive load of αSyn in the dopaminergic neurons of the SN[2]. It is important to consider that, in addition to the hαSyn expression induced by AAV-mediated transduction, the endogenous mouse αSyn also contributes to the load of total αSyn expression. Transgenic mice over-expressing mouse αSyn develop similar synuclein pathology, neuropathology, and motor impairment to those mouse models based on the overexpression of hαSyn[32]. Regarding microglial activation, the present mouse model might be used to study how different molecular and cellular players such as cytokines, neurotransmitters, astrocytes, neurons, the blood-brain barrier, and T cells might regulate the acquisition of pro-inflammatory or anti-inflammatory functional phenotypes[8,10,11]. This model also constitutes an important tool for studying the role of the peripheral immune system, including not only T cells but also macrophages, monocytes, and neutrophils, on the processes of neuroinflammation and neurodegeneration of nigral neurons[11,33,34]. Finally, this mouse model also represents a valuable system to study the cellular and molecular mechanisms of neurodegeneration in vivo, including those induced by internal cellular processes, such as oxidative stress, energy deficits, and damaged organelles [2], or those exerted by external players, such as neurotoxic factors produced by microglial cells, astrocytes, and cytotoxic T cells[8,28,29,35].

A limitation of this mouse model is the study of how the pathological aggregation of αSyn in extra-cerebral locations might constitute the initial stages in the development of Parkinson's disease[36]. In this regard, there is growing evidence indicating that, before the neurodegeneration of nigral neurons and motor impairment, αSyn pathology begins in the gut mucosa and the olfactory epithelium[36] and, probably, the αSyn-specific T-cell response as well[12]. Afterward, αSyn aggregates would migrate through the vagus nerve to the brain stem, triggering the neuroinflammation and neurodegeneration of dopaminergic neurons[12]. Although the AAV-hαSyn model recapitulates most aspects of Parkinson's disease, there is no evident involvement of the pathological aggregation of αSyn in extra-cerebral locations in this model. An alternative model involving hαSyn pathology appropriate for studying these aspects of Parkinson's disease might be transgenic mice overexpressing hαSyn under the control of the Thy1 promoter, the Thy1-*SNCA* model[37], in which disease development is dependent on the gut microbiota and involves an evident gastrointestinal impairment[38].

Although it is helpful for the study of the diverse processes associated with the pathophysiology of Parkinson's disease, the present mouse model involves critical steps that should

be minutely checked, including the correct delivery of the viral vectors in the corresponding spatial coordinates, the selective expression of hαSyn in neurons (which depends on the AAV serotype and the vector construct), and the proper AAV dose and timing before analyzing the Parkinsonian phenotype. The analysis of the proper delivery of the viral vectors in the SN is necessary, as the usage of the correct spatial coordinates of the SN might not be enough when the needle is not entirely straight, which is sometimes imperceptible to the human eye. Moreover, the diffusion of the AAV vectors depends on the AAV serotype[39]. For these reasons, it is necessary to perform periodical quality controls checking the correct delivery and diffusion of the injected AAV-GFP vectors following the observation of GFP in brain slices containing the area of the SN.

Regarding the selective expression of hαSyn in neurons, in principle, the expression of hαSyn could be engineered to be controlled by a promoter selective for neurons or, even more precise, selective for dopaminergic neurons, such as the use of the TH promoter in AAV vectors to induce the selective expression of genes in dopaminergic neurons[40]. However, this strategy does not work when what is sought is overexpression of the gene of interest. For this reason, in the present model, it is essential to use a strong promoter (a promoter inducing high expression of the downstream gene) and AAV serotypes with neuronal tropism. In this study, the CBA promoter was used as a strong promoter to induce the overexpression of hαSyn, and the AAV5 serotype was used for the viral vector. This serotype has been used before to transduce mouse and rat neurons[41,42]. Here, the results demonstrated that, 12 weeks after the delivery of AAV5-GFP in the SN of mice, the green fluorescence was selectively present on the ipsilateral side of both the SN and striatum (**Figure 1**), indicating the efficient transduction of neurons of the nigrostriatal pathway.

Another critical aspect of this mouse model of Parkinson's disease is the time point required to analyze a particular process after surgery. In this regard, this work shows a kinetic study of different processes involved in the pathology. Since key time points change with the dose of viral genomes given per mouse, the serotype of AAV used, or even with the batch of AAV used, a dose-response analysis of the amount of AAV-αSyn required to induce a significant loss of TH+ neurons and motor impairment was first carried out. Previous studies have shown significant motor impairment and a loss of TH+ neurons of the nigrostriatal pathway after 12 weeks of AAV-αSyn injections in mice at doses ranging from 6×10^8–3×10^{10} viral genomes per mouse[16,17,30,31]. Accordingly, the dose of AAV-hαSyn used to induce the hαSyn expression in the nigrostriatal pathway, the loss of TH^+ neurons, and motor impairment in mice ranged from 1×10^8–1×10^{10} viral genomes per mouse. Moreover, to control that the loss of TH^+ neurons and motor impairment were induced by the overexpression of hαSyn in the SN and not by AAV infection of neurons of the SN, control groups were included in which AAV coding for a reporter gene (AAV-eGFP) was delivered unilaterally in the SN of mice and neurodegeneration and motor impairment were determined. The results showed that, 12 weeks after the stereotaxic surgery, 1×10^{10} viral genomes per mouse was a proper dose of AAV5-hαSyn, as mice receiving this viral load displayed significant hαSyn in the nigrostriatal pathway (**Figure 2** and **Figure 3**), loss of TH+ neurons (**Figure 4**), and motor impairment (**Figure 5**). In contrast, lower doses of AAV5-hαSyn (1×10^8 viral genomes per mouse and 1×10^9 viral genomes per mouse) were not strong enough to reach significant changes in all these parameters together (**Figures**

2–4). Of note, the administration of AAV-GFP at 1 x 10^{10} viral genomes per mouse induced a low (~20%), but significant degree of loss of TH^+ neurons of nigral dopaminergic neurons (**Figure 4A,B**). This result agrees with previous observations using this model[41] and is probably the consequence of a low level of neuroinflammation induced by the administration of AAV vectors in the SN. Nevertheless, the extent of loss of TH^+ neurons was significantly higher in mice receiving AAV5-hαSyn compared with those receiving the same dose of AAV-GFP (**Figure 4C**). Of note, the kinetics of hαSyn expression not only depend on the efficiency of transduction but also on the extent of AAV diffusion[39]. Since AAV diffusion depends on the AAV serotype, the precise key time points in this animal model may vary when using another AAV serotype different from AAV5.

Afterward, a kinetic analysis was conducted using 1 x 10^{10} viral genomes per mouse to determine key time points in this mouse model. Since current evidence has shown some early symptoms that appear before motor impairment, which would allow the early diagnosis of Parkinson's disease[43,44], these experiments sought to find the time point at which hαSyn expression was already evident but in the absence of motor impairment. The results show that the onset of hαSyn expression in the SN was at 5 weeks after the stereotaxic delivery of AAV-hαSyn (**Figure 6**). This time point constitutes an interesting temporal point to start administering therapies tailored to stop the neuroinflammatory and neurodegenerative processes. Other key time points determined here were the peak times for two critical events associated with the neuroinflammation process: the time at which microglia reach the maximal degree of activation and the time of maximal T-cell infiltration into the SN. The results showed a curve with a trend reaching two waves of maximal microglial activation, the first one at 10 weeks after the surgery and the second one at 15 weeks after the surgery (**Figure 7**). The kinetic analysis of T-cell infiltration showed the peak time of Treg infiltration into the SN at 11 weeks after the stereotaxic surgery (**Figure 8**). Surprisingly, no effector T cells ($CD4^+$ $Foxp3^-$) were detected infiltrating the SN during the time frame analyzed (weeks 8–13 after surgery). Altogether, these results suggest a proper frame of time to start administering therapies geared toward stopping the process of neuroinflammation and attenuating T-cell infiltration into the SN using this preclinical model, which ranges between week 5 after surgery (the onset of hαSyn overexpression) and week 10 after surgery (the first wave of neuroinflammation and T-cell infiltration) (**Figure 9**).

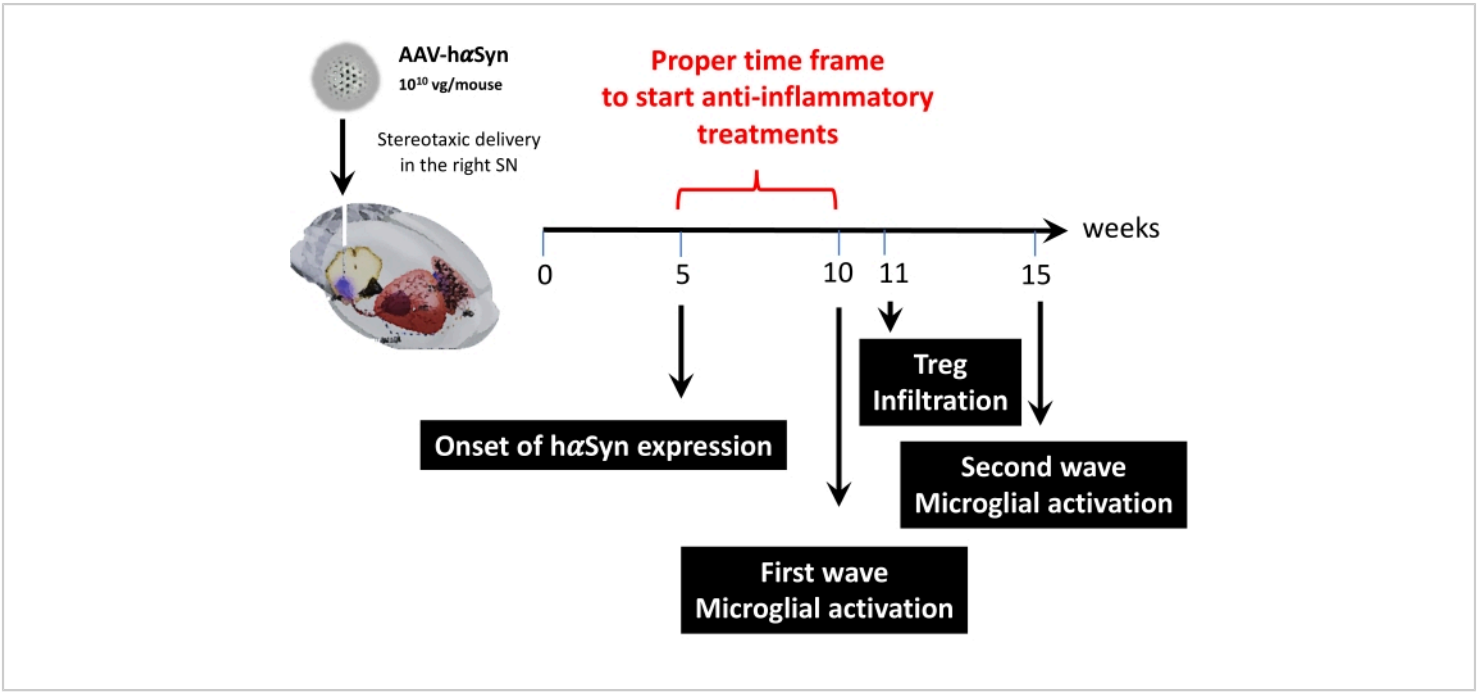

Figure 9: Summary of the key time points found for this animal model. Please click here to view a larger version of this figure.

Disclosures

The authors declare that the research was conducted in the absence of any financial or non-financial competing interests.

Acknowledgments

We thank Dr. Sebastián Valenzuela and Dr. Micaela Ricca for their valuable veterinary assistance in our animal facility. This work was supported by "Financiamiento Basal para Centros Científicos y Tecnológicos de Excelencia de ANID" Centro Ciencia & Vida, FB210008 (to Fundación Ciencia & Vida), and the Geroscience Center for Brain Health and Metabolism, FONDAP-15150012. This work was also funded by grants FONDECYT-1210013 (to R.P.) and FONDECYT-1150766 (to F.C.) from "Agencia Nacional de Investigación y Desarrollo de Chile (ANID)" and MJFF-10332.01 (to R.P.) and MJFF-17303 (to F.C.) from the Michael J Fox Foundation for Parkinson's Research.

References

1. Braak, H. et al. Staging of brain pathology related to sporadic Parkinson's disease. *Neurobiology of Aging.* **24** (2), 197-211 (2003).
2. Lim, K. L., Zhang, C. W. Molecular events underlying Parkinson's disease - An interwoven tapestry. *Frontiers in Neurology.* **4**, 33 (2013).
3. Abdelmotilib, H. et al. α-Synuclein fibril-induced inclusion spread in rats and mice correlates with dopaminergic neurodegeneration. *Neurobiology of Disease.* **105**, 84-98 (2017).
4. Mori, F. et al. Relationship among alpha-synuclein accumulation, dopamine synthesis, and

neurodegeneration in Parkinson disease substantia nigra. *The Journal of Neuropathology & Experimental Neurology.* **65** (8), 808-815 (2006).

5. Winklhofer, K. F., Haass, C. Mitochondrial dysfunction in Parkinson's disease. *Biochimica et Biophysica Acta.* **1802** (1), 29-44 (2010).
6. Vazquez-Velez, G. E., Zoghbi, H. Y. Parkinson's disease genetics and pathophysiology. *Annual Review of Neuroscience.* **44**, 87-108 (2021).
7. Dehay, B. et al. Lysosomal impairment in Parkinson's disease. *Movement Disorders.* **28** (6), 725-732 (2013).
8. Gonzalez, H., Elgueta, D., Montoya, A., Pacheco, R. Neuroimmune regulation of microglial activity involved in neuroinflammation and neurodegenerative diseases. *Journal of Neuroimmunology.* **274** (1-2), 1-13 (2014).
9. Pacheco, R. T-cell based immunotherapies for Parkinson's disease. *Exploration of Neuroprotective Therapy.* **1** (2), 72-85 (2021).
10. Gonzalez, H., Contreras, F., Pacheco, R. Regulation of the neurodegenerative process associated to Parkinson's disease by CD4+ T-cells. *Journal of Neuroimmune Pharmacology.* **10** (4), 561-575 (2015).
11. Gonzalez, H., Pacheco, R. T-cell-mediated regulation of neuroinflammation involved in neurodegenerative diseases. *Journal of Neuroinflammation.* **11** (1), 201 (2014).
12. Campos-Acuna, J., Elgueta, D., Pacheco, R. T-cell-driven inflammation as a mediator of the gut-brain axis involved in Parkinson's disease. *Frontiers in Immunology.* **10**, 239 (2019).
13. Blesa, J., Phani, S., Jackson-Lewis, V., Przedborski, S. Classic and new animal models of Parkinson's disease. *Journal of Biomedicine and Biotechnology.* **2012**, 845618 (2012).
14. Ulusoy, A., Decressac, M., Kirik, D., Bjorklund, A. Viral vector-mediated overexpression of alpha-synuclein as a progressive model of Parkinson's disease. *Progress in Brain Research.* **184**, 89-111 (2010).
15. Gomez-Benito, M. et al. Modeling Parkinson's disease with the alpha-synuclein protein. *Frontiers in Pharmacology.* **11**, 356 (2020).
16. Song, L. K. et al. Targeted overexpression of alpha-synuclein by rAAV2/1 vectors induces progressive nigrostriatal degeneration and increases vulnerability to MPTP in mouse. *PLoS One.* **10** (6), e0131281 (2015).
17. Theodore, S., Cao, S., McLean, P. J., Standaert, D. G. Targeted overexpression of human alpha-synuclein triggers microglial activation and an adaptive immune response in a mouse model of Parkinson disease. *Journal of Neuropathology and Experimental Neurology.* **67** (12), 1149-1158 (2008).
18. Sanchez-Guajardo, V., Annibali, A., Jensen, P. H., Romero-Ramos, M. alpha-Synuclein vaccination prevents the accumulation of parkinson disease-like pathologic inclusions in striatum in association with regulatory T cell recruitment in a rat model. *Journal of Neuropathology and Experimental Neurology.* **72** (7), 624-645 (2013).
19. Sanchez-Guajardo, V., Febbraro, F., Kirik, D., Romero-Ramos, M. Microglia acquire distinct activation profiles depending on the degree of alpha-synuclein neuropathology in a rAAV based model of Parkinson's disease. *PLoS One.* **5** (1), e8784 (2010).
20. Oliveras-Salva, M. et al. rAAV2/7 vector-mediated overexpression of alpha-synuclein in

mouse substantia nigra induces protein aggregation and progressive dose-dependent neurodegeneration. *Molecular Neurodegeneration.* **8**, 44 (2013).

21. Cho, C. et al. Evaluating analgesic efficacy and administration route following craniotomy in mice using the grimace scale. *Scientific Reports.* **9** (1), 359 (2019).
22. Flecknell, P. *Laboratory Animal Anaesthesia.* 3rd Ed. (ElsevierAcademic Press. Cambridge, MA (2009).
23. Bind, R. H., Minney, S. M., Rosenfeld, S., Hallock, R. M. The role of pheromonal responses in rodent behavior: Future directions for the development of laboratory protocols. *Journal of the American Association for Laboratory Animal Science.* **52** (2), 124-129 (2013).
24. Paxinos, G., Franklin, K. B. J. *The Mouse Brain in Stereotaxic Coordinates.* Academic Press. Cambridge, MA (2001).
25. Elgueta, D. et al. Dopamine receptor D3 expression is altered in CD4+ T-cells from Parkinson's disease patients and its pharmacologic inhibition attenuates the motor impairment in a mouse model. *Frontiers in Immunology.* **10**, 981 (2019).
26. Gage, G. J., Kipke, D. R., Shain, W. Whole animal perfusion fixation for rodents. *Journal of Visualized Experiments.* (65), e3564 (2012).
27. Fernandez-Suarez, D. et al. The monoacylglycerol lipase inhibitor JZL184 is neuroprotective and alters glial cell phenotype in the chronic MPTP mouse model. *Neurobiology of Aging.* **35** (11), 2603-2616 (2014).
28. Elgueta, D. et al. Pharmacologic antagonism of dopamine receptor D3 attenuates neurodegeneration and motor impairment in a mouse model of Parkinson's disease. *Neuropharmacology.* **113** (Pt A), 110-123 (2017).
29. Montoya, A. et al. Dopamine receptor D3 signalling in astrocytes promotes neuroinflammation. *Journal of Neuroinflammation.* **16** (1), 258 (2019).
30. Williams, G. P. et al. Targeting of the class II transactivator attenuates inflammation and neurodegeneration in an alpha-synuclein model of Parkinson's disease. *Journal of Neuroinflammation.* **15** (1), 244 (2018).
31. Benskey, M. J. et al. Silencing alpha synuclein in mature nigral neurons results in rapid neuroinflammation and subsequent toxicity. *Frontiers in Molecular Neuroscience.* **11**, 36 (2018).
32. Rieker, C. et al. Neuropathology in mice expressing mouse alpha-synuclein. *PLoS One.* **6** (9), e24834 (2011).
33. Harms, A. S. et al. alpha-Synuclein fibrils recruit peripheral immune cells in the rat brain prior to neurodegeneration. *Acta Neuropathologica Communications.* **5** (1), 85 (2017).
34. Williams, G. P. et al. CD4 T cells mediate brain inflammation and neurodegeneration in a mouse model of Parkinson disease. *Brain.* **144** (7), 2047-2059 (2021).
35. Matheoud, D. et al. Intestinal infection triggers Parkinson's disease-like symptoms in Pink1(-/-) mice. *Nature.* **571** (7766), 565-569 (2019).
36. Jan, A., Goncalves, N. P., Vaegter, C. B., Jensen, P. H., Ferreira, N. The prion-like spreading of alpha-synuclein in Parkinson's disease: Update on models and hypotheses. *International Journal of Molecular Sciences.* **22** (15), 8338 (2021).

37. Chesselet, M. F. et al. A progressive mouse model of Parkinson's disease: The Thy1-aSyn ("Line 61") mice. *Neurotherapeutics.* **9** (2), 297-314 (2012).

38. Sampson, T. R. et al. Gut microbiota regulate motor deficits and neuroinflammation in a model of Parkinson's disease. *Cell.* **167** (6), 1469-1480.e12 (2016).

39. Ciron, C. et al. Human alpha-iduronidase gene transfer mediated by adeno-associated virus types 1, 2, and 5 in the brain of nonhuman primates: Vector diffusion and biodistribution. *Human Gene Therapy.* **20** (4), 350-360 (2009).

40. Ben-Shaanan, T. L. et al. Activation of the reward system boosts innate and adaptive immunity. *Nature Medicine.* **22** (8), 940-944 (2016).

41. Albert, K., Voutilainen, M. H., Domanskyi, A., Airavaara, M. AAV vector-mediated gene delivery to substantia nigra dopamine neurons: Implications for gene therapy and disease models. *Genes.* **8** (2), 63 (2017).

42. Bordia, T., Perez, X. A., Heiss, J., Zhang, D., Quik, M. Optogenetic activation of striatal cholinergic interneurons regulates L-dopa-induced dyskinesias. *Neurobiology of Disease.* **91**, 47-58 (2016).

43. Kim, A. et al. Upgraded methodology for the development of early diagnosis of Parkinson's disease based on searching blood markers in patients and experimental models. *Molecular Neurobiology.* **56** (5), 3437-3450 (2018).

44. Lei, H. et al. Parkinson's disease diagnosis via joint learning from multiple modalities and relations. *IEEE Journal of Biomedical and Health Informatics.* **23** (4), 1437-1449 (2018).